THE JOURNAL OF NAVIGATION (2006), **59**, 307–320. © The Royal Institute of Navigation
doi:10.1017/S0373463306003699 Printed in the United Kingdom

High Accuracy Pseudolite-based Navigation System: Compensating for Right-Hand Circularly Polarized Effect

Haeyoung Jun and Changdon Kee

(*Seoul National University*, *Republic of Korea*)
(Email: hyjun@snu.ac.kr, kee@snu.ac.kr)

This paper presents further research on the SNUGL pseudolite-based navigation system presented in this journal in 2003. This system has centimetre-level accuracy, but has an error source arising from right-hand circularly polarized (RHCP) transmissions, unlike outdoor Global Positioning System (GPS). The GPS satellites and pseudolites use RHCP signals, and the polarization affects carrier-phase measurements according to the Line-of-Sight (LOS) vectors from transmitters to receivers. The RHCP error is eliminated by a double differencing process in outdoor GPS, but the error remains in the pseudolite-based system because the LOS vectors from transmitters to a reference and user receivers are different for the close transmitter constellations. This paper shows the RHCP effect on the pseudolite-based navigation system through simulations and experiments. It then shows the RHCP-compensation method improves the measurement and position accuracy by over 10%.

KEY WORDS

1. GPS 2. Pseudolite 3. Indoor Navigation 4. RHCP

1. INTRODUCTION. GPS is a good sensor for navigation, but it cannot be used indoors or in signal-blocked environments, even though there are many potential users in such environments. Many approaches have been tested for indoor navigation using GPS technologies, and a pseudolite-based navigation system can be a solution. With such motivation, the Seoul National University GPS Lab (SNUGL) implemented an indoor navigation system using asynchronous pseudolites in 1999 [Kee, Jun et al. 2000] and published a description in this journal [Kee, Jun and Yun, 2003]. This system uses pseudolites as transmitters and a reference and user receivers, and has an accuracy of several centimetres. This system can be used for outdoor navigation with or without GPS satellites. The error sources of the system, in general, include multipath, pseudolite position error, and measurement noise (thermal noise). There exists, however, one more antenna-related error source, which has been ignored for GPS but should be considered in

https://doi.org/10.1017/S0373463306003699 Published online by Cambridge University Press

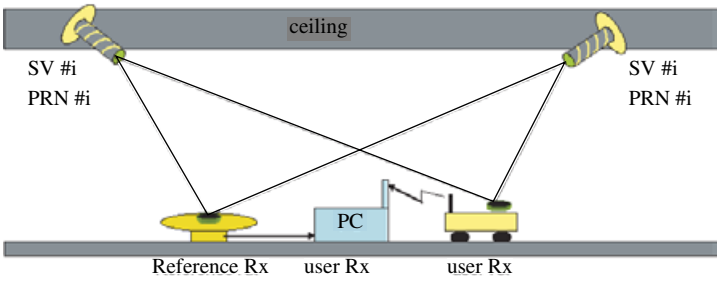


Figure 1. SNUGL pseudolite-based indoor navigation system overview.

pseudolite-based navigation systems. That is the Right Hand Circularly Polarized (RHCP) effect. This affects carrier-phase double-difference measurements because of the different line of sight (LOS) vectors between two receivers and two transmitters. Generally the LOS vectors are the same for the outdoor GPS system because the transmitters are very far away from the receivers, but pseudolites are so close to the receivers that the LOS vectors are different for two receivers, even from the same transmitter.

The RHCP effect on GPS with non-aligned antenna arrays was introduced by Lightsey [Lightsey and Parkinson, 1996]. Lawrence [Lawrence and Cobb, 1995] and Zimmerman [Zimmerman, 1996] extended the RHCP effect to an indoor navigation system with non-aligned antenna arrays. Adams modified the RHCP equations to remove an ambiguity and also analysed RHCP effects with non-aligned antenna arrays in an indoor navigation system [Adams and How, 1998].

This paper analyses the RHCP effects on the carrier-phase double-difference measurements and on the Carrier-phase Differential GPS (CDGPS) solutions of the SNUGL asynchronous pseudolite-based navigation system even with aligned antennas, and compares experimental results with simulation results. This paper also proposes an RHCP-compensating method for improving the accuracy of the pseudolite-based navigation system.

2. THEORY.

2.1. *SNUGL Pseudolite-based Navigation System.* The pseudolite-based navigation system makes it possible for users to navigate in urban canyons and even inside buildings. The system is composed of pseudolites, transmission antennas, receiver antennas, a reference receiver, user receivers, wireless modems, and a processing computer, as shown in Figure 1.

Transmission antennas, which are right-hand circularly polarized, are installed beneath the ceiling and connected to pseudolites. The user and the reference receivers gather integrated carrier-phase (ICP) measurements and send them to the PC via wireless modems. The PC then solves the navigation equations with ICP double differences and the CDGPS algorithm. The distances between pseudolites and the receivers are very short, tens of metres or less. Thus, a user movement causes a rapid change of the line of sight (LOS) vectors from the pseudolites to the user. Moreover, in contrast to the outdoor GPS, the two LOS vectors from one pseudolite to the reference and to the user are different from each other. The different LOS vectors

https://doi.org/10.1017/S0373463306003699 Published online by Cambridge University Press

Table 1. Average Positioning Error of the Pseudolite-based Navigation System (1σ).

	Near the reference station	Whole test area
3-Dimensional RMS Error	1·56 cm	4·3 cm

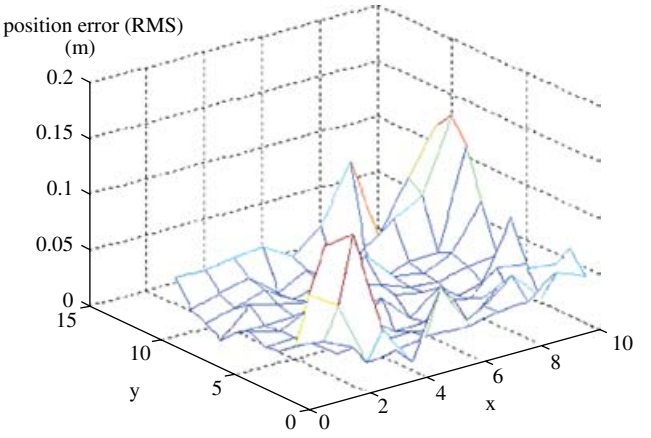


Figure 2. SNUGL Pseudolite-based Navigation System Position Error (RMS) with a Reference Station at (0, 0, 0).

bring about the RHCP effect on the carrier-phase double-difference measurements and solutions shown in Figure 2 and Table 1. The position error increases as a user moves farther from a reference because the LOS vector difference at a greater distance is larger than that close-by. The RHCP effect on the measurement is very small; below several centimetres, however, it may not be negligible because the noise level and the navigation error of the system are not much bigger than the RHCP effect.

2.2. *Right-Hand Circularly Polarized* (*RHCP*) *Effect*. GPS satellites and pseudolites use Right-Hand Circularly Polarized signals. The signal is an E-field radiating from a transmitter to a receiver, which is circularly polarized perpendicularly to the direction of propagation as shown in Figure 3. When the signal is received by a patch antenna, the phase measurement is calculated by the projection of the E-field onto coordinates fixed to the receiver antenna. The carrier-phase measurement on a patch antenna can be modelled as a combination of two perpendicular components with a phase delay of 90 degrees, so phase measurements even for the same distances can be different depending on the receiving angle. Therefore, the RHCP effect can be ignored only if the two receiving antennas have the same bore-sight direction and the LOS vectors from the transmitter to the two receiving antennas are the same, because the RHCP effects on the reference and the user are then identical and eliminated through the double differencing process. In the outdoor GPS, the LOS vectors from a satellite to a reference and a user are almost equal and are not changed by user movements as shown in Figure 4(a). Therefore, it is not necessary

https://doi.org/10.1017/S0373463306003699 Published online by Cambridge University Press

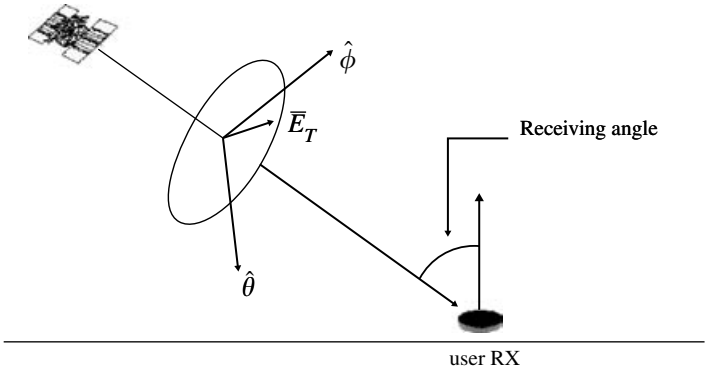


Figure 3. Right-hand circularly polarized GPS signal E-field.

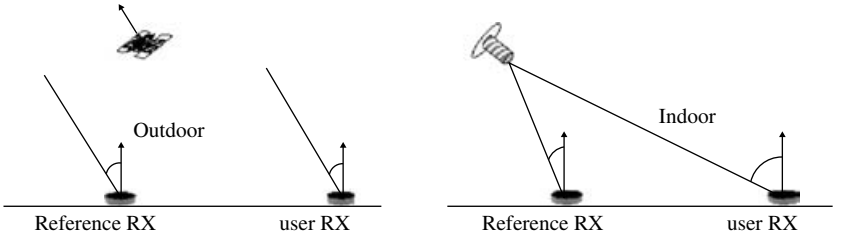


Figure 4. The LOS vectors for a reference and a user receiver are the same in outdoor GPS (a), but different in the pseudolite-based navigation system, depending on the user position (b).

for outdoor GPS users to consider the RHCP effect, except for some special users who use non-aligned antenna arrays. On the other hand, pseudolite-based navigation system users should not disregard the RHCP effect, even when a user antenna is aligned with a reference antenna, because the LOS vectors from a pseudolite to the reference and the user are different depending on the user position as shown in Figure 4(b).

2.3. *Coordinate System and Rotation Matrix*. For our analysis, two coordinate systems are defined. One coordinate $(\hat{x}'', \hat{y}'', \hat{z}'')$ is fixed on the transmitter antenna and the $\hat{z}''$-axis points in the direction of signal propagation $(\bar{A}_x + \bar{A}_y + \bar{A}_z)$. The other coordinate is the inertial coordinate $(\hat{X}, \hat{Y}, \hat{Z})$, in which the $\hat{Z}$-axis is toward the zenith. Figure 5 shows the coordinate systems. $(\hat{x}', \hat{y}', \hat{z}')$ is a transient coordinate.

The rotation matrix, $R_{(Inertial \rightarrow Tx)}$, from the inertial coordinate to the transmitter-fixed coordinate can be calculated by a two-step rotation transformation. First, the inertial coordinate is rotated by α degrees about the $\hat{X}$-axis to a transient coordinate $(\hat{x}', \hat{y}', \hat{z}')$ so that the $\hat{Z}$-axis is parallel to the vector $(\bar{A}_y + \bar{A}_z)$, where $\bar{A}$ is defined as a LOS vector from a transmitter to a receiver. Second, the coordinate $(\hat{x}', \hat{y}', \hat{z}')$ is rotated by β degrees about the $\hat{y}'$-axis so that the $\hat{z}'$-axis is parallel to the vector $\bar{A}$. The result is the transmitter-fixed coordinate $(\hat{x}'', \hat{y}'', \hat{z}'')$. Thus, the rotation matrix,

https://doi.org/10.1017/S0373463306003699 Published online by Cambridge University Press

R_T, from the transmitter-fixed coordinate to the inertial coordinate can be calculated from equation (1).

$$
\begin{aligned}
R_{T(Tx\rightarrow Inertial)} &= (R_{(Inertial\rightarrow Tx)})^T \\
&= (R(2,\beta)\ R(1,\alpha))^T \\
&= \left[\begin{bmatrix} cos\beta & 0 & -sin\beta \\ 0 & 1 & 0 \\ sin\beta & 0 & cos\beta \end{bmatrix}\begin{bmatrix} 1 & 0 & 0 \\ 0 & cos\alpha & sin\alpha \\ 0 & -sin\alpha & cos\alpha \end{bmatrix}\right]^T \\
&= \begin{bmatrix} cos\beta & 0 & sin\beta \\ sin\alpha sin\beta & cos\alpha & -sin\alpha cos\beta \\ -cos\alpha sin\beta & sin\alpha & cos\alpha cos\beta \end{bmatrix} \\
&= \begin{bmatrix} \dfrac{\sqrt{A_y^2+A_z^2}}{|\bar{A}|} & 0 & \dfrac{A_x}{|\bar{A}|} \\ \dfrac{-A_xA_y}{|\bar{A}|\sqrt{A_y^2+A_z^2}} & \dfrac{A_z}{\sqrt{A_y^2+A_z^2}} & \dfrac{A_y}{|\bar{A}|} \\ \dfrac{-A_xA_z}{|\bar{A}|\sqrt{A_y^2+A_z^2}} & \dfrac{-A_y}{\sqrt{A_y^2+A_z^2}} & \dfrac{A_z}{|\bar{A}|} \end{bmatrix}
\end{aligned}
\tag{1}
$$

where the rotation angles α and β can be defined by equation (2).

$$
\begin{aligned}
cos\alpha &= -\frac{z}{\sqrt{y^2+z^2}} = \frac{A_z}{\sqrt{A_y^2+A_z^2}} \\
sin\alpha &= \frac{y}{\sqrt{y^2+z^2}} = \frac{-A_y}{\sqrt{A_y^2+A_z^2}} \\
cos\beta &= \frac{\sqrt{y^2+z^2}}{\sqrt{x^2+y^2+z^2}} = \frac{\sqrt{A_y^2+A_z^2}}{|\bar{A}|} \\
sin\beta &= \frac{-x}{\sqrt{x^2+y^2+z^2}} = \frac{A_x}{|\bar{A}|}
\end{aligned}
\tag{2}
$$

2.4. *RHCP Phase Error Modelling*. The instantaneous field of a plane wave shown in Figure 6, travelling toward the Z-axis, can be written as equation (3) and

https://doi.org/10.1017/S0373463306003699 Published online by Cambridge University Press

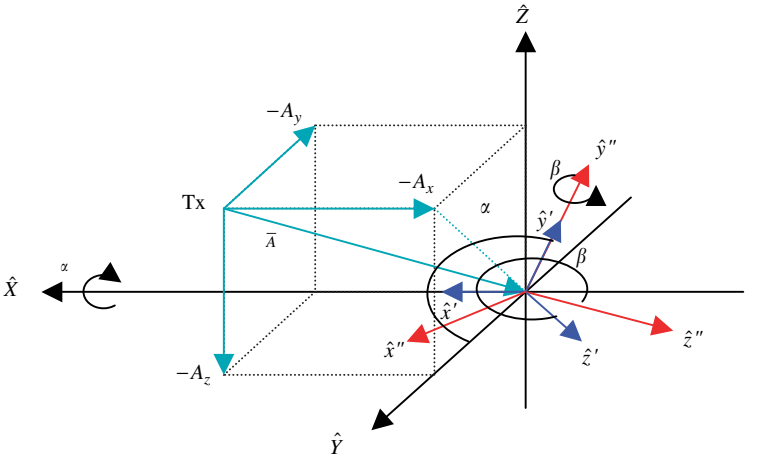


Figure 5. Two Coordinate Systems. $(\hat{x}, \hat{y}, \hat{z})$ is an inertial coordinate and $(\hat{x}'', \hat{y}'', \hat{z}'')$ is a transmitter-fixed coordinate.

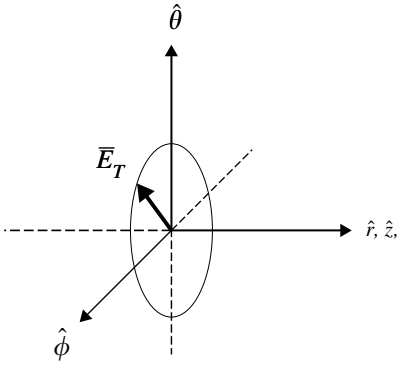


Figure 6. E-field vector radiated from a helical antenna.

simplified as equation (4) with respect to the transmitter-fixed coordinates.

$$\bar{E}(z;t) = E_\theta(z;t)\hat{\theta} + E_\phi(z;t)\hat{\phi},$$
$$\textit{where}$$
$$E_\theta(z;t) = E_{\theta 0}cos(\omega t + kz + \phi_x)$$
$$E_\phi(z;t) = E_{\phi 0}cos(\omega t + kz + \phi_y) \tag{3}$$
$$\Delta\phi = \phi_y - \phi_x = -\left(\frac{1}{2} + 2n\right)\pi, \quad n = 0, 1, 2, \ldots$$

$$\bar{E}_T = E_\theta\hat{\theta} + E_\phi\hat{\phi} + E_r\hat{r} = \begin{bmatrix} cos(\omega_{L1}t) \\ sin(\omega_{L1}t) \\ 0 \end{bmatrix} \tag{4}$$

The received E-field is represented as $\bar{E}_{rec}$ with respect to the receiver-fixed coordinate and calculated as equation (5). If the bore sight of the receiver antenna is

https://doi.org/10.1017/S0373463306003699 Published online by Cambridge University Press

pointed toward the zenith, the tilt angle can be assumed to be zero, therefore, the receiver-fixed coordinates are the same as the inertial coordinates and $R_v = R_{ANT} = I$ (the identity matrix), where R_v is the rotation matrix from the vehicle to the inertial frame, and R_{ANT} is the rotation matrix from the receiver antenna to the vehicle frame. The zero tilt angle indicates the best condition for minimizing the RHCP effect.

$$\begin{aligned}\bar{E}_{rec} &= T_{T-rec}\bar{E}_T = (R_V R_{ANT})^T R_T \bar{E}_T \\ &= \begin{bmatrix} T_{11} & T_{12} & T_{13} \\ T_{21} & T_{22} & T_{23} \\ T_{31} & T_{32} & T_{33} \end{bmatrix} \begin{bmatrix} cos(\omega_{L1}t) \\ sin(\omega_{L1}t) \\ 0 \end{bmatrix} = \begin{bmatrix} T_{11}cos(\omega_{L1}t) + T_{12}sin(\omega_{L1}t) \\ T_{21}cos(\omega_{L1}t) + T_{22}sin(\omega_{L1}t) \\ T_{31}cos(\omega_{L1}t) + T_{32}sin(\omega_{L1}t) \end{bmatrix},\end{aligned}$$

where (5)

$R_V = Rotation\ Matrix\ from\ vehicle\ to\ inertial\ coordinate$

$R_{ANT} = Rotation\ Matrix\ from\ Rx\ antenna\ to\ vehicle\ coordinate$

$R_T = Rotation\ Matrix\ from\ Tx\ antenna\ to\ inertial\ coordinate$

$T_{T-rec} = Rotation\ Matrix\ from\ Tx\ antenna\ to\ Rx\ coordinate$

The patch antenna on the receiver can be considered as two dipole antennas in the X and the Y direction with a phase delay of 90 degrees [Balanis, 1997]; therefore, the received signal can be modelled by equation (6). The integrated carrier-phase measurement is calculated by integrating the phase measurement, and should be $\omega_{L1}t$, ideally, instead of $[\omega_{L1}t\text{-}arctan(b/a)]$. The unexpected additional phase term, $arctan(b/a) = arctan(\frac{T_{21}+T_{12}}{T_{11}-T_{22}})$ in equations (6) and (7) represents a phase delay caused by the RHCP effect.

$$\begin{aligned} r(t) &= E_x^{REC}(t) + E_y^{REC}(t - 2\pi/(4\omega_{L1})) \\ &= T_{11}cos(\omega_{L1}t) + T_{12}sin(\omega_{L1}t) \\ &\quad + T_{21}cos(\omega_{L1}t - \pi/2) + T_{22}sin(\omega_{L1}t - \pi/2) \\ &= T_{11}cos(\omega_{L1}t) + T_{12}sin(\omega_{L1}t) + T_{21}sin(\omega_{L1}t) - T_{22}cos(\omega_{L1}t) \\ &= (T_{11} - T_{22})cos(\omega_{L1}t) + (T_{21} + T_{12})sin(\omega_{L1}t) \\ &= (\sqrt{a^2 + b^2})cos[\omega_{L1}t - arctan(b/a)], \end{aligned} \tag{6}$$

where

$a = T_{11} - T_{22}$

$b = T_{21} + T_{12}$

$$\phi_{RHCP} = arctan\left(\frac{T_{21} + T_{12}}{T_{11} - T_{22}}\right) \tag{7}$$

3. SIMULATIONS OF THE RHCP EFFECT

3.1. *Unexpected Additional Measurement by RHCP Effect*. Figure 7 shows the unexpected additional phase measurement from the RHCP effect simulated with

https://doi.org/10.1017/S0373463306003699 Published online by Cambridge University Press

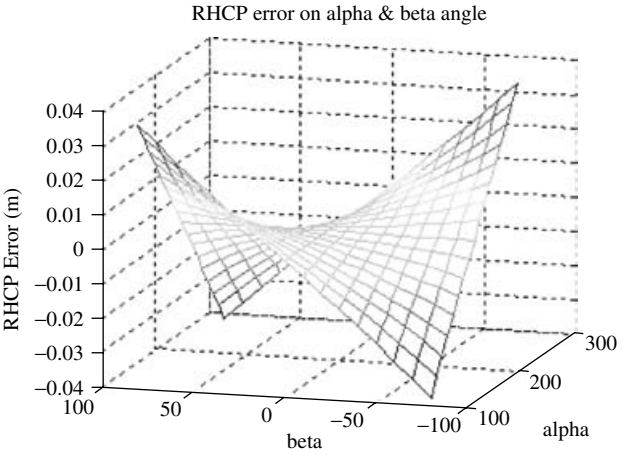


Figure 7. Simulated additional phase measurement by RHCP effect with various rotation angles.

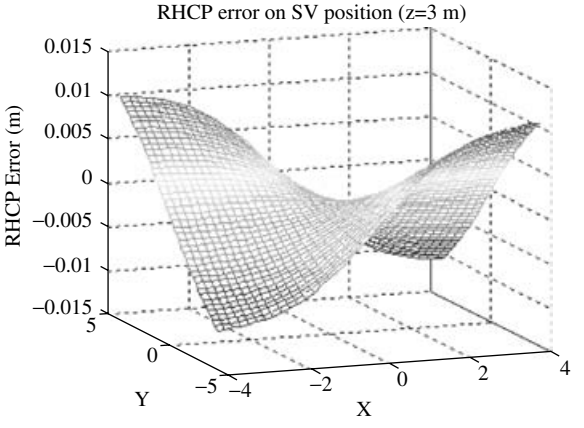


Figure 8. Simulated additional phase term on the single carrier-phase measurement by RHCP effect with a receiver at (0, 0, 0) and the pseudolite position varies about (x, y, 3).

various rotation angles α and β, which depend on the direction of radiation. The peak-to-peak difference is about 6 cm.

Low elevation angles of the pseudolites are not available in the actual system, therefore we consider the actual situation of a volume $10\text{ m} \times 10\text{ m} \times 3\text{ m}$, where the pseudolites are fixed on the top corners and the ceiling. Figure 8 shows the unexpected additional phase term on the single carrier-phase measurement from the RHCP effect at the position (0, 0, 0) when the pseudolite moves to (x, y, 3). The figure shows that the RHCP phase error depending on the position (not the orientation or attitude) is as big as ± 1 cm, and can be bigger when the measurements are double-differenced.

3.2. *RHCP Effect on the Pseudolite-based Navigation System.* The SNUGL pseudolite-based indoor navigation system uses double differences of carrier-phase measurements taken by a reference and a user receiver. If we assume the reference

https://doi.org/10.1017/S0373463306003699 Published online by Cambridge University Press

station is fixed at (0, 0, 0), which is the best position to remove system errors, the RHCP effects on the double-difference measurements can be simulated in various combinations of the pseudolite and the user positions indicated by (x, y), as shown in Figure 9. Figure 9(a) shows the result when two pseudolites are at opposite corners and the distance is the longest. Figure 9(b) shows the result when two pseudolites are on the same side, and Figure 9(c) shows the result when the master pseudolite is at the centre.

Such RHCP errors in the double-difference measurements are introduced into the user position, which is calculated using these measurements. Figure 10 shows the simulated RHCP effects on the CDGPS 3-dimensional solutions as root mean square (RMS) values, which are as high as several centimetres. Consequently, the RHCP error on the solution is not negligible compared with the noise level of the system, and it is important that the RHCP error is not white noise but a bias error.

4. EXPERIMENTAL RESULTS.

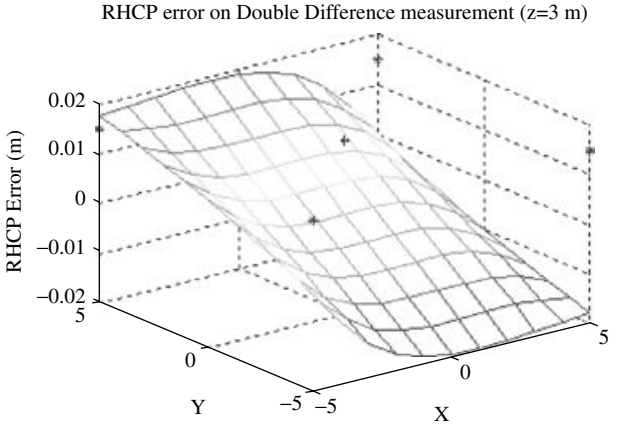
4.1. *Experimental RHCP Errors on the Carrier-phase Measurements.* Carrier-phase double-difference measurements for two receivers and two pseudolites were compared with the double difference of the actual ranges. For the comparison, the positions of the reference and the user logging points were pre-measured on the floor, and the positions of the transmitter antennas were surveyed using the Inverse CDGPS (ICDGPS) method [Kee, Yun, Jun and Parkinson, 1999]. Carrier-phase measurements are logged for 100 epochs at each of 110 positions on the floor, from $-1{\cdot}5$ to 1·5 metres on the X-axis and from $-1{\cdot}2$ to 1·5 metres on the Y-axis on a 30-cm grid, as shown in Figure 11. The RHCP effects are very small when the user is close to the reference station at (0, 0, 0); therefore, the pseudolite positions were solved using ICP data measured in the area close to the reference station, to minimize the RHCP effect on the pseudolite positions themselves. The calculated pseudolite positions are shown in Table 2.

Figure 12 shows the RHCP errors on the double-difference measurements simulated using the same situation as the actual test setup when PL2 and PL4 are used. The experimental results of the differences between the measurements and the actual ranges, which are the measurement errors, are plotted in Figure 12(b). It is clear that the simulated RHCP errors in Figure 12(a) and the experimental result in Figure 12(b) have the same tendency. They show similar slant planes and the inclinations can be considered as the RHCP effect. The same tendency is shown in other pseudolite combinations.

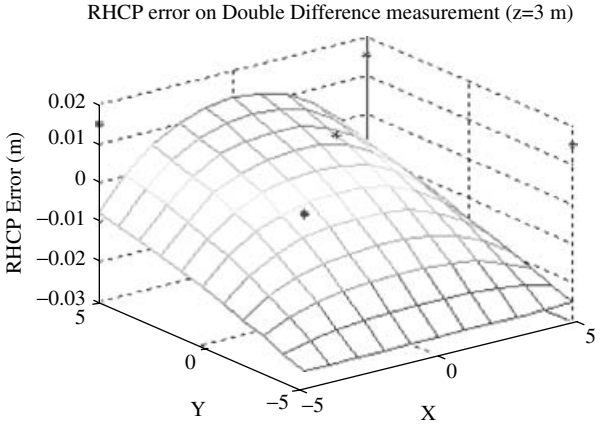
4.2. *RHCP Compensation Results.* We can simulate the RHCP effects using the reference, user and pseudolite positions, and the RHCP effects can be removed by compensating simulated values. Figure 13 shows the result of the compensation. The compensated double-difference measurements have no inclination or bias errors.

Table 3 and Figure 14 show the compensation results. The average RMS errors, which were measured at 110 user positions with all pseudolite combinations, are reduced from 1·06 cm to 0·98 cm for a 7·4% improvement, and the position accuracy is improved by 11·6%. The values are not very large because another error source, multipath, is a dominant error source compared with the RHCP effects. The small

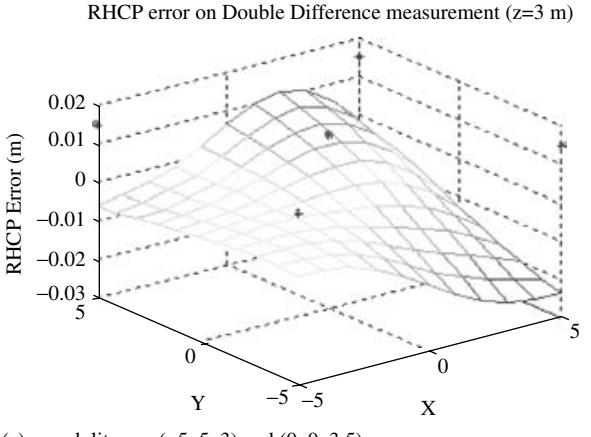
https://doi.org/10.1017/S0373463306003699 Published online by Cambridge University Press



(a) pseudolites on (−5, 5, 3) and (5, −5, 3)



(b) pseudolites on (−5, 5, 3) and (−5, −5, 3)



(c) pseudolites on (−5, 5, 3) and (0, 0, 3.5)

Figure 9. Simulated RHCP error on the carrier-phase double difference for a reference at (0, 0, 0), users at (x, y, 0) and two pseudolites (a) at (−5, 5, 3) and (5, −5, 3), (b) at (−5, 5, 3) and (−5, −5, 3), and (c) at (−5, 5, 3) and (0, 0, 3.5).

https://doi.org/10.1017/S0373463306003699 Published online by Cambridge University Press

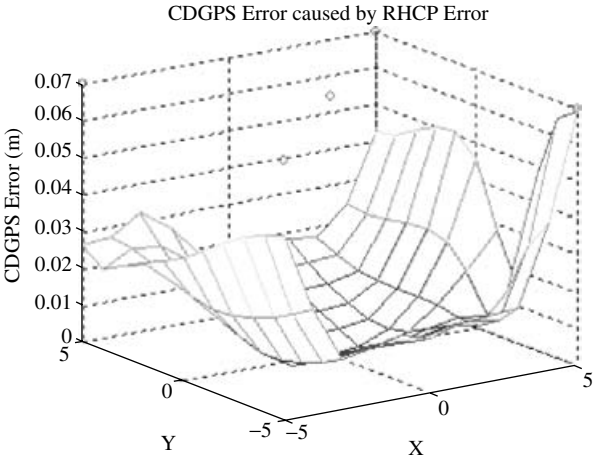


Figure 10. Simulated RHCP effect on the CDGPS solution of the users at (x, y, 0).

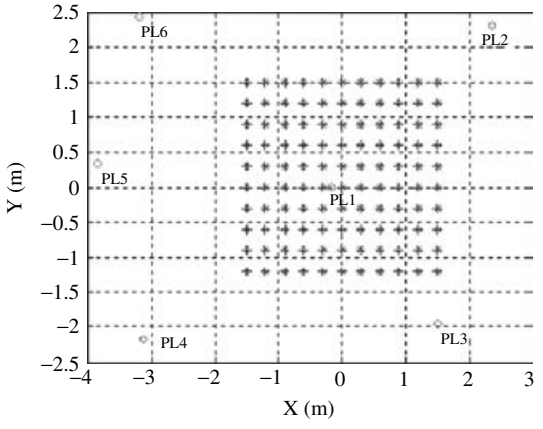


Figure 11. Experimental setup. Circles are pseudolite positions and '*'s are the user positions where the carrier-phase measurements are logged.

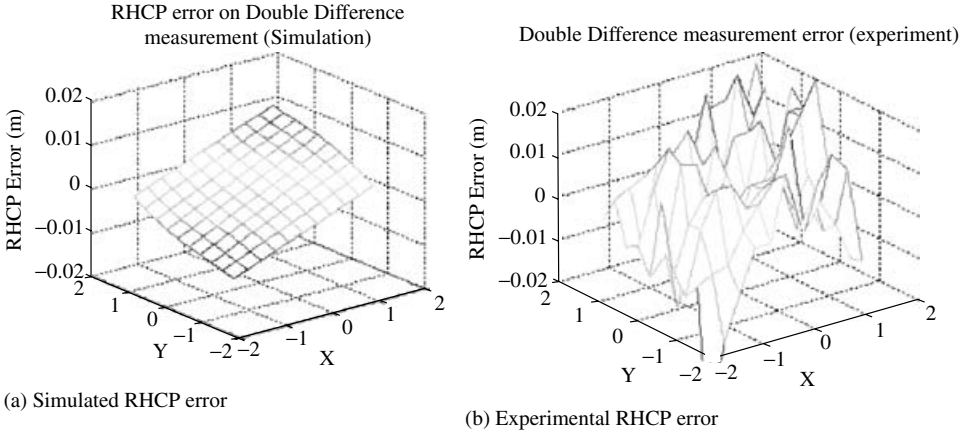
test area is a bad environment for multipath errors. The system errors are not proportional to the application size, but the multipath errors can be reduced when the application volume is larger. Therefore, the RHCP-compensation would be more effective in larger system application areas.

If the user stands near the reference station, the LOS vectors from the pseudolites to the user and to the reference receivers are similar and the RHCP effects on double-difference measurements are very small. As the user moves away from the reference, the RHCP effects become larger. This means the improvement would be larger for users at greater distances from the reference station. Figure 15 shows how much the measurements are improved after RHCP-compensation. When the user is 1·8 m from the reference station, the measurements are improved by 15·1%, and the position improvement in this area also was better than 15%.

https://doi.org/10.1017/S0373463306003699 Published online by Cambridge University Press

Table 2. Calculated pseudolite positions.

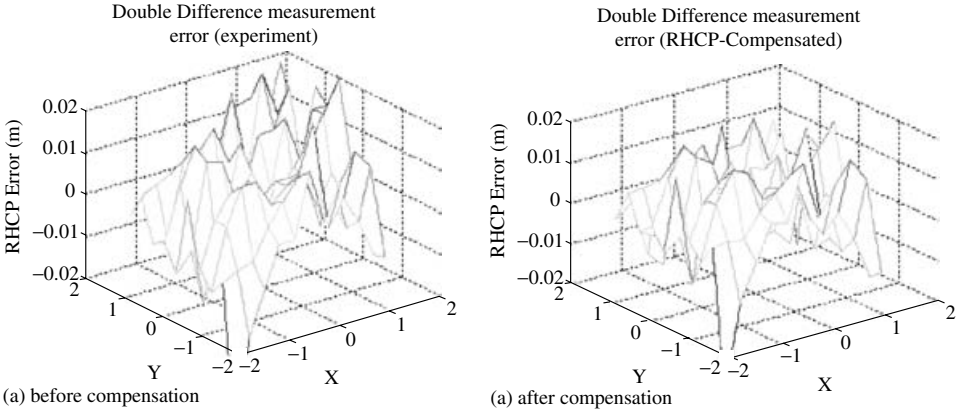
	PL 1	PL 2	PL 3	PL 4	PL 5	PL 6
X (m)	−0·149	2·374	1·524	−3·843	−3·843	−3·179
Y (m)	−0·001	2·307	−1·972	−2·189	0·325	2·428
Z (m)	2·423	2·292	2·287	2·320	2·368	2·310



(a) Simulated RHCP error

(b) Experimental RHCP error

Figure 12. (a) Simulated and (b) Experimental RHCP error on the double-difference measurements with PL2 at (2.37, 2.31, 2.29) and PL4 at (–3.13, −2.19, 2.32).



(a) before compensation

(a) after compensation

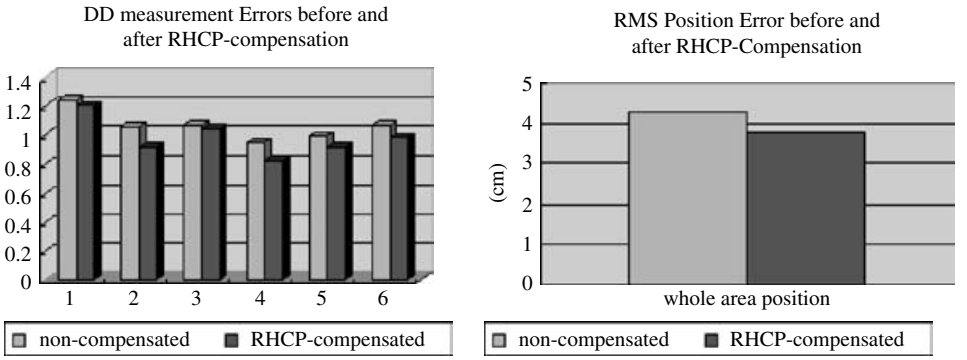
Figure 13. RHCP-compensated errors on the double-difference measurements with PL2 at (2.37, 2.31, 2.29) and PL4 at (−3.13, −2.19, 2.32).

5. CONCLUSIONS. LOS vectors from GPS satellites to a reference station and users are almost the same in outdoor GPS. That is why RHCP effects have been ignored, even in precise positioning. On the other hand, the RHCP effect should be considered in a pseudolite-based navigation system, because the LOS vectors from pseudolites to a user change as the user moves while the LOS vectors

https://doi.org/10.1017/S0373463306003699 Published online by Cambridge University Press

Table 3. Measurements and Position Accuracy Improvement after RHCP Compensation.

	DD1	DD2	DD3	DD4	DD5	position
Before (cm)	1·24	1·05	1·06	0·94	0·99	4·3
After (cm)	1·20	0·91	1·04	0·82	0·91	3·8
Improvement	3·2%	13·3%	1·9%	12·8%	8·1%	11·6%



(a) measurement improvements (b) position improvement

Figure 14. Measurements and Position Accuracy Improvement after RHCP Compensation.

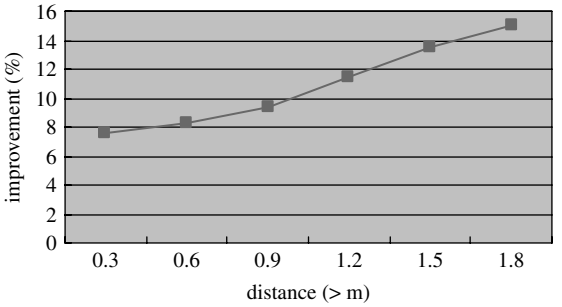


Figure 15. DD measurement improvement after RHCP-compensation as a user moves away from a reference.

to a reference are fixed. Figure 14 shows the experimental results measured by the SNUGL asynchronous pseudolite-based indoor navigation system. The RHCP effect is not very large but should not be ignored, because the noise level of the pseudolite-based navigation system is also very small. The RHCP effect is as big as the system noise level, and moreover, it is a bias error. We can obtain more accurate precise positioning by compensating the RHCP effect. After compensation, the RMS error of the double-difference measurements was reduced by 7·3% on average, and reduced by 15% when the user is far from the reference. This improvement affects the position accuracy, and the position accuracy is improved by 11·6% on average. Users should therefore compensate for the RHCP effects for

https://doi.org/10.1017/S0373463306003699 Published online by Cambridge University Press

a more accurate pseudolite-based navigation system. This high accuracy pseudolite-based navigation system could be used for factory automation or an indoor attitude determination system, and should be more accurate than non-compensated systems.

ACKNOWLEDGEMENTS

This research was supported in part by a grant from the BK-21 Program for Mechanical and Aerospace Engineering Research at Seoul National University.
This research was supported in part by ETRI.

REFERENCES

Adams, J. and How, J. (1998). GPS Attitude determination for spinning spacecraft with non-aligned antenna arrays. *Proceedings of ION NTM-98*, Long Beach, CA.

Balanis, C. (1997). *Antenna Theory*, 2nd edition, John Wiley & Sons.

Kee, C., Jun H., and Yun, D. (2003). Indoor navigation system using asynchronous pseudolites. *The Journal of Navigation*, **56**, 443–455.

Kee, C., Jun, H., Yun, D., Kim, B., Kim, Y., Parkinson, B., Langenstein, T., Pullen, S. and Lee, J. (2000). Development of indoor navigation system using asynchronous pseudolites. *Proceedings of ION GPS–2000*, Salt Lake City, UT.

Kee, C., Yun, D., Jun, H., Parkinson, B., Langenstein, T., and Pullen, S. (1999). Precise calibration of pseudolite positions in indoor navigation systems. *Proceedings of ION GPS–99*, Nashville, TN.

Kee, C., Yun, D., and Jun, H. (2003). Precise calibration method of pseudolite positions in indoor navigation systems. *Computers & Mathematics with Applications*, **46**, 1711–1724.

Lawrence, D., Cobb, H. (1995). Maintaining GPS positioning in steep turns using two antennas. *Proceedings of ION GPS-95*, Palm Springs, CA.

Lightsey, E., Parkinson, B. (1996). GPS-based attitude determination on nonaligned antenna arrays. *Proceedings of ION GPS-96*, Kansas City, MO.

Zimmerman, K. (1996). *Experiments in the Use of the Global Positioning System for Space Vehicle Rendezvous*, Ph.D. dissertation, Stanford University.

https://doi.org/10.1017/S0373463306003699 Published online by Cambridge University Press